Magnetohydrodynamic (MHD) Complex Flow Generation in Microchannel

Dong Sung Kim and Tai Hun Kwon

Department of Mechanical Engineering, Pohang University of Science and Technology (POSTECH), San 31 Hyoja-dong Nam-gu, Pohang, Kyunbuk, 790-784, South Korea, smkds@postech.ac.kr & thkwon@postech.ac.kr

ABSTRACT

In this paper, we present a design methodology for *magnetohydrodynamic (MHD) complex flow* generation inside a simple straight microchannel in which electrodes are patterned on two side walls and a bottom wall. The Lorentz force, a driving force to generate a flow, can be variously induced in the microchannel by changing applied voltages at the patterned electrodes and a magnetic field. The required applied *voltage conditions* at each electrode to generate *axial*, *transverse*, *sinusoidal* and *multi-vortical flows* are discussed for a given magnetic field. Three-dimensional CFD (computational fluid dynamics) simulations confirm the successful generations of the designed complex flows in the microchannel. The design methodology for the present MHD complex flows such as sinusoidal or vortical flow might be applied to precise control or mixing of the flow inside the microchannel.

Keywords: complex flow, computational fluid dynamics (CFD), design methodology, magnetohydrodynamics (MHD), microfluidics

1 INTRODUCTION

The fluid flow control is inherently required in microfluidic systems [1]. The magnetohydrodynamic pumping allows a bi-directional flow in the microchannel without moving parts and requires very low voltages for propulsion, which is compatible with biological samples [2-6]. In this regards, the MHD flow control was successfully applied to the biological applications of lab-on-a-chips, e.g., continuous flow PCR (polymerase chain reaction) [5].

When a conducting fluid is placed under the external electric and magnetic fields, a Lorentz force is generated in the perpendicular direction to both the electric and magnetic fields (**F**=**J**×**B**, where **F**, **J** and **B** are the Lorentz force, electric current density and magnetic flux density, respectively). The Lorentz force acts as a body force to the fluid and therefore, the fluid flow can be generated without the use of a pressure drop. The previous reported studies, however, were limited in simple two-dimensional flows, i.e., an axial flow [2-5] or a transverse one [6].

In this study, the generations of incompressible MHD complex flows inside a simple straight microchannel in which electrodes are patterned on two side walls and a bottom wall have been extensively investigated by means of CFD simulations under the steady-state condition.

2 THEORY AND MODEL

2.1 Theory of Magnetohydrodynamics

If we neglect the effect of an electrically conducting fluid flow on the external electric and magnetic fields, the governing equations for an MHD flow can be derived from the classical fluid mechanics and electromagnetics:

$$\mathbf{J} = \sigma(\mathbf{E} + \mathbf{u} \times \mathbf{B}) \tag{1}$$

$$\nabla \cdot \mathbf{u} = 0 \tag{2}$$

$$\rho \frac{D\mathbf{u}}{Dt} = -\nabla p + \mu \nabla^2 \mathbf{u} + \mathbf{J} \times \mathbf{B} \tag{3}$$

where σ, **E**, **u**, ρ, μ, t and p are electric conductivity, electric field, fluid velocity, density and viscosity of fluid, time and pressure, respectively. Equations (1-3) represent Ohm's law, mass continuity of an incompressible fluid and Navier-Stokes equation as a momentum conservation equation including the Lorentz force (**J**×**B**), respectively.

2.2 Model of MHD Microchannel

Figure 1 shows a schematic configuration of a straight microchannel in which electrodes are patterned on two side walls and patterned on a bottom wall periodically, designed in this study. We assumed that a constant magnetic field, **B**, is applied in +z-direction over the microchannel. The applied DC (direct current) voltages at the side wall electrodes are denoted by V_{w1} and V_{w2}. At the electrodes patterned on the bottom wall, the DC voltages of V_{b1} and V_{b2} are assumed to be periodically applied as indicated in Figure 1. We suppose that $V_{w1} \geq V_{w2}$ and $V_{b1} \geq V_{b2}$ without loss of generality.

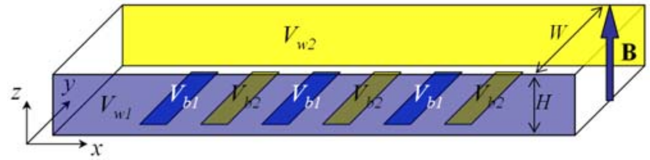

Figure 1: Schematic diagram of a MHD straight microchannel designed in this study. The microchannel contains two side wall electrodes (applied voltages of V_{w1} and V_{w2}) and bottom wall electrodes (periodically applied voltages of V_{b1} and V_{b2}). A constant magnetic field of **B** is applied over the microchannel in +z-direction.

3 DESIGN OF COMPLEX FLOWS

In this study, we assumed that there is no pressure difference between the inlet and outlet of the microchannel, i.e., $\nabla p=0$ in Equation (3), in order to observe the effect of Lorentz force on the flow only.

According to Equation (3) under the condition of constant **B** and $\nabla p=0$, one can generate various directions and magnitudes of the Lorentz forces by changing applied voltage conditions at the patterned electrodes (V_{w1}, V_{w2}, V_{b1} and V_{b2}) inside the microchannel shown in Figure 1. In this study, four different types of MHD flows are discussed based on the induced Lorentz forces: axial, transverse, sinusoidal and multi-vortical flows.

(i) *Axial flow*. When there is only voltage applied at the side wall electrodes without the bottom wall voltage, i.e., $V_{w1}>V_{w2}$ & $V_{b1}=V_{b2}=0$, the electric current density, J_{w1w2} is only generated in $+y$-direction according to Equation (1) and thereby the Lorentz force, F_{w1w2} is induced in $+x$-direction under the magnetic field in $+z$-direction as shown in Figure 2. Therefore, an axial flow is generated by the induced Lorentz force inside the microchannel as like in the previous results [2-5].

(ii) *Transverse flow*. Under the applied voltage condition of $V_{w1}=V_{w2}=0$ & $V_{b1}>V_{b2}$, the electric current density, J_{b1b2} is generated in $+x$- and $-x$-directions between the electrodes V_{b1} and V_{b2} and between V_{b2} and V_{b1}, respectively. Therefore, the Lorentz force, F_{b1b2} is induced in $-y$- and $+y$-directions according to the generated J_{b1b2} under the given **B** in $+z$-direction as depicted in Figure 3, thereby resulting in a transverse flow in the microchannel as like in [6].

(iii) *Sinusoidal flow*. For the case of $V_{w1}>V_{w2}$, $V_{b1}>V_{b2}$, $V_{w1}=V_{b1}$ and $V_{w2}=V_{b2}$, the current densities, J_{w1w2} in $+y$-direction (between the electrodes V_{w1} and V_{w2}), J_{b1b2} in $+x$-direction (between V_{b1} and V_{b2}) and J_{b1b2} in $-x$-direction (between V_{b2} and V_{b1}) are generated. Furthermore, between the electrodes V_{b1} and V_{w2} and between V_{w1} and V_{b2}, J_{b1w2} and J_{w1b2}, respectively, are generated in $+y$-direction. Therefore, for the given **B** in $+z$-direction, one can obtain the Lorentz forces, F_{w1w2}, F_{b1w2} and F_{w1b2} induced in $+x$-direction and F_{b1b2} induced in $\pm y$-directions inside the microchannel as indicated in Figure 4.

It might be noted here that due to the voltage condition of $V_{w1}=V_{b1}$ and $V_{w2}=V_{b2}$, there is no electric current density and Lorentz force induced between the electrodes V_{w1} and V_{b1} and between V_{w2} and V_{b2}. And also, the magnitudes of the induced Lorentz forces, F_{b1w2} and F_{w1b2} are similar to each other. Based on the induced Lorentz forces, one can expect a sinusoidal flow generated in the microchannel.

(iv) *Multi-vortical flow*. Under $V_{w1}>V_{w2}$, $V_{b1}>V_{b2}$, $V_{w1}<V_{b1}$ and $V_{w2}=V_{b2}$, one can expect that the current densities, J_{w1w2} in $+y$-direction (between the electrodes V_{w1} and V_{w2}), J_{b1b2} in $+x$-direction (between V_{b1} and V_{b2}), J_{b1b2} in $-x$-direction (between V_{b2} and V_{b1}), J_{b1w2} in $+y$-direction (between V_{b1} and V_{w2}) and J_{w1b2} in $+y$-direction (between V_{w1} and V_{b2}) are generated. In this case, the current density of J_{b1w1} is also generated in $-y$-direction between the electrodes V_{w1} and V_{b1} since $V_{w1}<V_{b1}$. For the given magnetic field in $+z$-direction, the Lorentz forces, F_{w1w2}, F_{b1w2} and F_{w1b2} in $+x$-direction, F_{b1b2} in $\pm y$-directions and F_{b1w1} in $-x$-direction can be achieved in the microchannel as indicated in Figure 5.

It might be noted that, in this case, an electric current density and a Lorentz force are not induced between the electrodes V_{w2} and V_{b2} due to the voltage condition of $V_{w2}=V_{b2}$ and also there are an electric current density, J_{b1w1} and a Lorentz force, F_{b1w1} induced between the electrodes V_{w1} and V_{b1} due to the condition of $V_{w1}<V_{b1}$. Moreover, J_{b1w2} and F_{b1w2} have the largest magnitudes among the generated electric current densities and the induced Lorentz forces, respectively, since $V_{b1}>V_{w1}>V_{w2}$ under the given voltage condition.

It should be also noted that the induced Lorentz forces, F_{b1w2} ($+x$-direction), F_{b1b2} ($-y$-direction), F_{b1w1} ($-x$-direction) and F_{b1b2} ($+y$-direction) over the bottom electrode, V_{b1}, cause clockwise momentum thereby generating clockwise vortex flows near the bottom electrodes. Therefore, with the induced Lorentz forces in this case, one can achieve a globally sinusoidal flow containing localized multiple vortices, i.e., a multi-vortical flow.

Table 1 lists all possible required voltage conditions to achieve the four different types of MHD flows, i.e., axial, transverse, sinusoidal and multi-vortical flows inside the microchannel as discussed above.

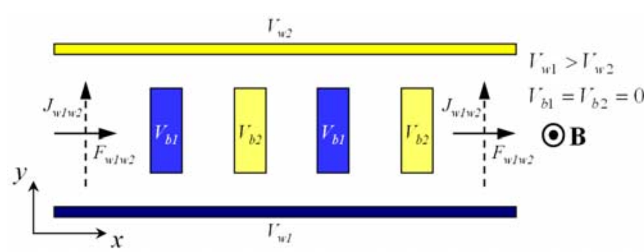

Figure 2: MHD axial flow: schematic diagram of induced electric current densities (broken arrows) due to the indicated applied voltages and the corresponding Lorentz forces (solid arrows) in the microchannel.

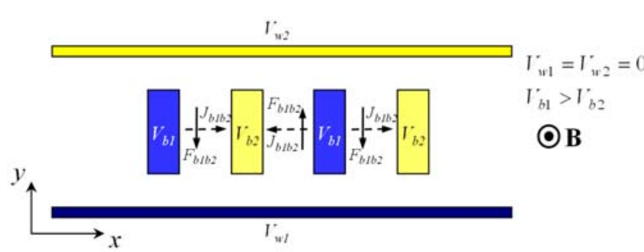

Figure 3: MHD transverse flow: schematic diagram of induced electric current densities (broken arrows) due to the indicated applied voltages and the corresponding Lorentz forces (solid arrows) in the microchannel.

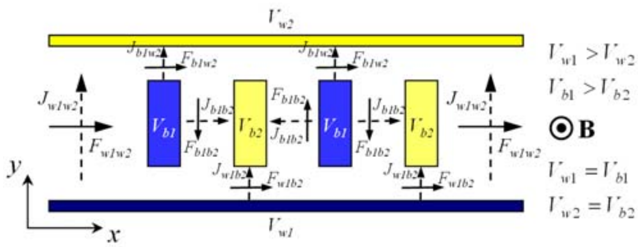

Figure 4: MHD sinusoidal flow: schematic diagram of induced electric current densities (broken arrows) due to the indicated applied voltages and the corresponding Lorentz forces (solid arrows) in the microchannel.

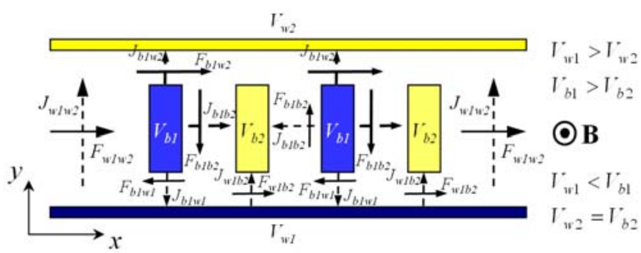

Figure 5: MHD multi-vortical flow: schematic diagram of induced electric current densities (broken arrows) due to the indicated applied voltages and the corresponding Lorentz forces (solid arrows) in the microchannel.

Flow type	Voltage condition
Axial flow	$V_{w1} > V_{w2}$ and $V_{b1} = V_{b2} = 0$
Transverse flow	$V_{w1} = V_{w2} = 0$ and $V_{b1} > V_{b2}$
Sinusoidal flow	$V_{w1} > V_{w2}$, $V_{b1} > V_{b2}$, $V_{w1} = V_{b1}$ and $V_{w2} = V_{b2}$
Multi-vortical flow	$V_{w1} > V_{w2}$, $V_{b1} > V_{b2}$ and $V_{w1} < V_{b1}$ & $V_{w2} \geq V_{b2}$ or $V_{w1} \leq V_{b1}$ & $V_{w2} > V_{b2}$

Table 1: Various MHD flow types and the corresponding required voltage conditions assuming $V_{w1} \geq V_{w2}$ and $V_{b1} \geq V_{b2}$ without loss of generality.

4 NUMERICAL ANALYSIS

In order to evaluate the proposed design methodology for the four different types of MHD flow generation inside the microchannel, three-dimensional CFD simulations under the steady-state condition were conducted based on the finite volume method with the governing equations of Equations (1-3) by means of CFD-ACE+ (CFD Research Corp., AL, USA).

In the CFD simulations, a microchannel was designed based on the model of the MHD microchannel depicted in Figure 1. The designed microchannel has two inlets and one outlet for a working fluid (Figure 6). The width, height and length of the microchannel were designed to be 500μm, 200μm and 2.3mm, respectively. The electrodes were patterned on the whole area (200μm×2.3mm) of both side channel walls. On the bottom wall, 8 electrodes having the size of 100μm×400μm were patterned periodically with an interval between the adjacent electrodes of 100μm starting from 400μm away from the inlet. It might be mentioned that, in this case, the interval between the base of the side wall electrodes and the bottom wall electrodes became 50μm.

The physical properties of sea water were chosen as those of the working fluid. The density, dynamic viscosity, electric conductivity, relative permeability and relative permittivity of sea water were 1025kg m^{-3}, 1.09×10^{-3}kg m^{-1} s^{-1}, $4\Omega^{-1}$ m^{-1}, 1 and 72, respectively [2].

For flow boundary conditions, the same fixed pressure was assigned at the inlets and outlet to obtain no pressure difference according to the assumption in this study. On the whole channel wall, the no-slip condition was assigned. For electric boundary conditions, a DC voltage was applied at each patterned electrode according to the desired flow type based on Table 1. At the area other than the electrodes on the wall, the non-penetration condition of an electric current was assigned. Finally, it was assumed that a constant magnetic field with the magnitude of 0.2T was applied in +z-direction.

The applied voltage conditions for the four types of MHD flows in the CFD simulations and the corresponding simulation results are as follows.

(i) *Axial flow*. The boundary conditions of voltages applied at the electrodes are V_{w1}=20V, V_{w2}=V_{b1}=V_{b2}=0V based on the design methodology listed in Table 1. Figure 6 shows the result of the general MHD axial flow according to the applied boundary conditions in this case.

(ii) *Transverse flow*. The boundary conditions of voltages applied at the electrodes are V_{b1}=40V, V_{w1}=V_{w2}=V_{b2}=0V based on the design methodology listed in Table 1. An MHD transverse flow inside the microchannel was obtained from the applied boundary conditions as shown in Figure 7.

(iii) *Sinusoidal flow*. The boundary conditions of voltages applied at the electrodes are V_{w1}=V_{b1}=30V, V_{w2}=V_{b2}=0V based on the design methodology listed in Table 1. Figure 8 shows the result of an MHD sinusoidal flow induced by the applied boundary conditions in this case.

(iv) *Multi-vortical flow*. The boundary conditions of voltages applied at the electrodes are V_{w1}=20V, V_{b1}=40V, V_{w2}=V_{b2}=0V based on the design methodology listed in Table 1. An MHD multi-vortical flow consisting of a globally sinusoidal flow with multiple vortices inside the microchannel, as expected, was achieved from the applied boundary conditions as shown in Figure 9.

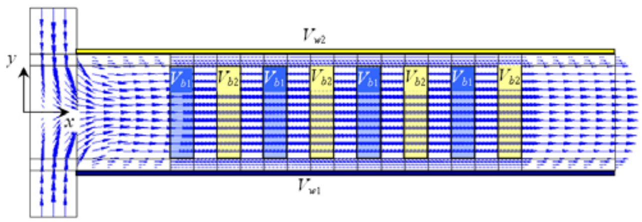

Figure 6: MHD axial flow: CFD simulation result when V_{w1}=20V and V_{w2}=V_{b1}=V_{b2}=0V under B=0.2T where W=500μm and H=200μm.

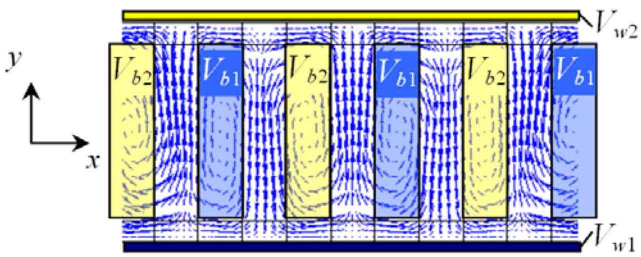

Figure 7: MHD transverse flow: CFD simulation result when V_{b1}=40V and V_{w1}=V_{w2}=V_{b2}=0V under B=0.2T.

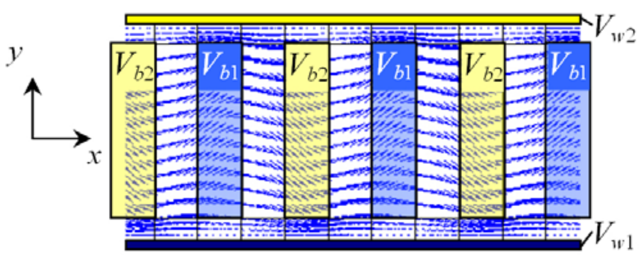

Figure 8: MHD sinusoidal flow: CFD simulation result when V_{w1}=V_{b1}=30V and V_{w2}=V_{b2}=0V under B=0.2T.

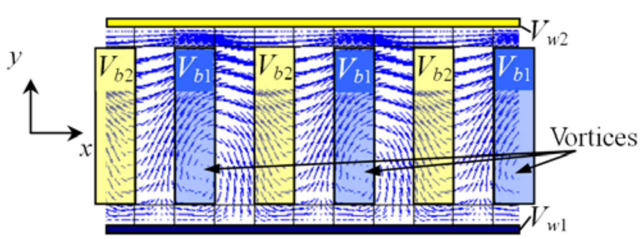

Figure 9: MHD multi-vortical flow: CFD simulation result when V_{w1}=20V, V_{b1}= 40V and V_{w2}=V_{b2}=0V under B=0.2T.

5 CONCLUDING REMARKS

In this study, we propose a design methodology for the generations of MHD complex flows inside a simple straight microchannel by inducing Lorentz forces in various directions and magnitudes. In the proposed model of a MHD microchannel, electrodes were patterned on two side walls and patterned on a bottom wall periodically. It was assumed that a constant magnetic field was applied over the microchannel. According to the design methodology proposed in this study, one can achieve an axial flow, a transverse flow, a sinusoidal flow and a multi-vortical flow that is composed of a globally sinusoidal flow with multiple vortices inside the same microchannel by simply changing the magnitudes of applied voltages on the patterned electrodes. Three-dimensional CFD simulations were conducted to evaluate the design methodology in this study. The CFD simulation results confirmed the design methodology for the four different MHD flow generations.

One can carry out multiple processes inside the same microchannel by changing flow characteristics of the MHD flows based on the proposed design methodology, such as, transporting, control or mixing [6,7] of fluids or samples in fluid.

ACKNOWLEDGEMENT

The authors would like to thank to the Korean Ministry of Commerce, Industry and Energy for the financial supports via a research project of Development of Next-Generation New Technology (Development of Intelligent Robot Technologies for Laboratory Medicine by Applying Biotechnology).

REFERENCES

[1] D.R. Reyes, D. Iossifidis, P.-A. Auroux and A. Manz, Anal. Chem., 74, 2632-2636, 2002.

[2] J. Jang and S.S. Lee, Sensor Actuat. A, 80, 84-89, 2000.

[3] A.V. Lemoff and A.P. Lee, Sensor Actuat. B, 63, 178-185, 2000.

[4] A. Homsy, S. Koster, J.C.T. Eijkel, A. van den Berg, F. Lucklum, E. Verpoote and N.F. de Rooji, Lab Chip, 5, 466-471, 2005.

[5] J. West, B. Karamata, B. Lillis, J.P. Gleeson, J. Alderman, J.K. Collins, W. Lane, A. Mathewson and H. Berney, Lab Chip, 2, 224-230, 2002.

[6] H.H. Bau, J. Zhong and M. Yi, Sensor Actuat. B, 79, 207-215, 2001.

[7] D.S. Kim, S.W. Lee, T.H. Kwon and S.S. Lee, J. Micromech. Microeng., 14, 798-805, 2004.